Eur. Phys. J. B **32**, 73–79 (2003)
DOI: 10.1140/epjb/e2003-00075-9

THE EUROPEAN PHYSICAL JOURNAL B

Propagation of waves and chaos in transmission line with strongly anharmonic dangling resonator

P. Zieliński[1,3,a], A. Kułak[2], L. Dobrzyński[3], and B. Djafari-Rouhani[3]

[1] The H. Niewodniezański Institute of Nuclear Physics, ul. Radzikowskiego 152, 30-342 Kraków, Poland
[2] Department of Electronics, Academy of Mining and Metallurgy, Al. Mickiwicza 30, 30-059, Kraków, Poland
[3] Laboratoire de Dynamique et Structure des Matériaux Moléculaires[b], UFR de Physique, Université de Lille I, 59655 Villeneuve d'Ascq Cedex, France

Received 14 March 2002 / Received in final form 25 November 2002
Published online 14 March 2003 –

Abstract. Delayed differential equation of motion with multiple lags is derived for an anharmonic stub resonator coupled to a monomode transmission line. Transmission and reflection coefficients are found analytically in the harmonic approximation. Nonlinear response of the system is analysed by an electric circuit obeying the same equations of motion. Enhanced second harmonic generation is found at the frequencies, which in the harmonic approximation correspond to the zeros of transmission. An aperiodic (chaotic) response is found mainly in the frequency range close to the resonance of the dangling resonator. Zeros of transmission and total transmissions are shown to be lifted by the anharmonicity nearly in the same frequency region. Higher harmonics are preferentially transmitted at the zero transmission points in the presence of anharmonicity.

PACS. 43.25.+y Nonlinear acoustics – 05.45.Tp Time series analysis – 68.35.Ja Surface and interface dynamics and vibrations

1 Introduction

Scattering of guided waves on objects of well-designed geometry is now extensively studied mainly in the context of modern microelectronic, optoelectronic and acoustic devices. Of particular interest are electronic systems based on Aharonov-Bohm effect where guided matter waves of electrons are scattered on a conducting ring driven by an external magnetic field [1–3]. Transmission probability of such rings shows strong oscillations as a function of the flux or, alternatively, of the incident energy. In fact, the phenomenon is related to successive zeros of transmission and total transmission points occurring at some particular sets of parameters. Concomitant of a zero of transmission is a discontinuity of phase of the transmitted wave so that this phase cannot be used to count the system's density of states [4]. Zeros of transmission occur also in optic, magnetic and acoustic devices [5–7]. The zeros of transmission are even more pronounced there because of a better coherence of the electromagnetic and acoustic waves. The simplest geometry showing this intriguing property is that of a transmission line, or equivalently of an elastic string, with a single dangling resonator [4–10]. The scheme of such a system considered in this work is shown in Figure 1.

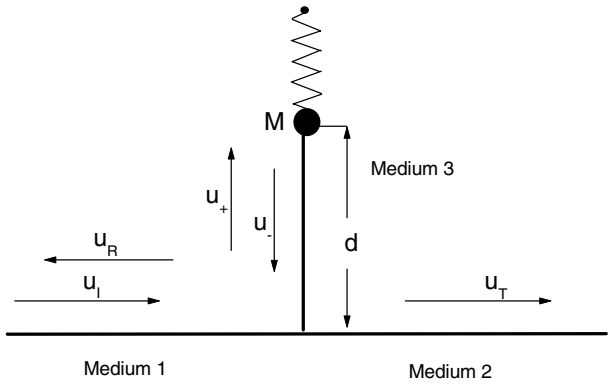

Fig. 1. Scheme of junction of three 1d monomode media with dangling anharmonic resonator. Anharmonic potential is represented by string. Arrows correspond to incident wave u_I and to related transmitted and reflected waves propagating in system.

Generally, a system showing zeros of transmission consists of a central resonator and of at least two leads or waveguides. One of the leads, "Medium 1" in Figure 1, conveys the incident and the reflected waves, u_I and u_R respectively. The other lead, "Medium 2" supports the outgoing wave u_T. The condition for a zero of transmission to occur at a given frequency is that there be a node at this frequency at the point where the outgoing lead is

[a] e-mail: Piotr.Zielinski@ifj.edu.pl
[b] CNRS ESA 8024

attached to the resonator. Then the attachment or detachment of the outgoing lead does not disturb the standing wave existing in the resonator. In the case of a stub dangling transmission line of Figure 1 this condition amounts to the completely destructive interference at the junction point between the waves u_+ and u_- propagating within the dangling part. It is interesting that zeros of transmission also occur in guides and resonators, which are not strictly one-dimensional but show a non-zero cross sections [8]. In turn, the condition for the total transmission (zero of reflection) is that the forces exerted by the waves existing within the resonator on the point where the ingoing waveguide joins the resonator be totally compensated by the force due the incident wave and transmitted wave. When the ingoing and outgoing leads connected to the dangling resonator of Figure 1 are identical, *i.e.* when the media 1 and 2 are the same, then the condition for the total transmission is that there be no force acting on the junction point from the resonator. In other words, there should be a maximum of the standing wave or a constructive interference at the junction point between the waves u_+ and u_- propagating in the resonator.

Formally it is also possible to distinguish another characteristic frequency at which there exist outgoing waves in the leads whereas there is no incident wave at all. This corresponds to a kind of eigenstate of the system. However, it has been shown [11,12] that a semi-infinite lead is equivalent to a damping so that this eigenstate is practically always damped and the corresponding frequency has a non-zero imaginary part. Therefore, this characteristic frequency does not play a significant role in the transmission and reflection and will not be considered here.

When the system is purely harmonic its equations of motion are linear and the frequency-domain response is readily given by the appropriate Green functions [13]. References [1,2,4–10] present various aspects of propagation of waves through different perfectly harmonic systems with dangling resonators. When arranged in a periodic array the dangling side resonators give rise to practically absolute stop bands even though the number of branches in the array might not exceed 10 [7]. A junction where three waveguides meet together [4,5,9], as shown in Figure 1, is the elementary constituent of all the branched systems. Noteworthy is that this kind of junction also underlies the design of the human and other mammal arterial system guiding the pulse tension waves [14,15].

The time domain behaviour of the general branched systems is governed by Volterra integro-differential equations [11] which result from the elimination of irrelevant degrees of freedom in analogy with the substrates' degrees of freedom in the gas-surface interaction problems [16,17]. Only in special cases of dispersionless and lossless semi-infinite waveguides do the equations of motion reduce to differential equations [11,12].

The purpose of this work is to study the influence of an anharmonicity located at the end of the dangling resonator on the propagation of waves in the system of Figure 1. In particular, the question addressed is how such an anharmonicity affects the zeros of transmission and the total transmission points. The location of anharmonicity at an end point is justified by microscopic considerations [11,12]. The atoms there have a better possibility to participate in large-amplitude motions in contrast to the inner atoms of the waveguides. Similarly, in macroscopic optic waveguides the end-points are the most plausible location of parasite, possibly non-linear, capacities inductances and resistances. In the present work an electric analogue circuit is used, which obeys equations of motion identical to the equations of motion of the mechanical system of Figure 1. Then a nonlinearity is placed in a capacitor which corresponds to a nonlinear potential.

The presence of an anharmonic element makes the description of the dynamics more involved. The frequency domain analysis does not apply since the response of the system comprises generally all the frequencies even if the external perturbation is purely monochromatic [11,18,19]. Thus, a systematic analysis of anharmonic systems must be based on time series obtained with a given external perturbation. In particular, the behaviour of the system under an oscillatory monochromatic external force is an analogue of the frequency domain response. A possibility of anharmonic elements to produce a chaotic response raises practical questions of how this kind of behaviour influences the propagation properties of the system.

2 Effective equations of motion for a stub anharmonic resonator

The triple junction with a stub resonator considered in this work is represented in Figure 1. It consists of three dispersionless one dimensional media (strings or transmission lines), of which parts 1 and 2 are semi-infinite whereas part 3 is a resonator of length d. All the media are monomode. The grafted part is terminated by a mass M placed in an anharmonic potential here represented by a string supposed anharmonic. Each line is characterised by its stiffness constant T_i and by its propagation velocity c_i. The corresponding wave impedances then are $\Gamma_i = T_i/c_i$.

The anharmonicity of the string depicted in Figure 1 has the mathematical form of the Duffing oscillator [18,19] so that the potential $V(u_M)$ due to the string is the following function of the displacement u_M of the mass M.

$$V(u_M) = \frac{1}{2}au_M^2 + \frac{1}{4}bu_M^4, \tag{1}$$

where a and b are some constants. With $a < 0$ and $b > 0$ the potential equation (1) shows a double well form considered in references [18,19]. Therefore, the present results are also important in the field of studies of a known nonlinear system with very specific dissipation. In the case of a single semi-infinite dispersionless and lossless waveguide attached to the mass M in the potential of equation (1) the system is readily equivalent to the damped Duffing oscillator [18,19].

In accordance with the geometry of Figure 1 the axis x is put horizontally, y vertically and the origin of axes lies at the junction point $x = y = 0$. The general response

of the system to an incident wave $u_I(x,t) = u_I(c_1t - x)$ arriving from the medium 1 consists of the following waves represented schematically in Figure 1: the transmitted wave $u_T(x,t) = u_T(c_2t - x)$, the reflected wave $u_R(x,t) = u_R(c_1t + x)$, and two waves propagating upwards and downwards in medium 3: $u_+(y,t) = u_+(c_3t - y)$ and $u_-(y,t) = u_-(c_3t + y)$.

The continuity of the wave field and the continuity of stress at the junction point implies the following boundary conditions at $x = y = 0$.

$$u_T = \alpha_1 u_I + \alpha_3 u_-, \quad u_R = \beta_1 u_I + \alpha_3 u_-, \quad u_+ = \alpha_1 u_I + \beta_3 u_- \tag{2}$$

at any time t, where α_i and β_i are given in terms of the wave impedances Γ_i $i = 1, 2, 3$

$$\alpha_i = \frac{2\Gamma_i}{\Gamma_1 + \Gamma_2 + \Gamma_3} \qquad \text{and} \qquad \beta_i = \alpha_i - 1. \tag{3}$$

The boundary condition at the end point of the medium 3, *i.e.* at $y = d$, is the Newton equation for the mass M in the potential $V(u_M)$ produced by the string

$$M\ddot{u}_M(t) + \frac{\partial V}{\partial u_M} = \Gamma_3(\dot{u}_+(d,t) - \dot{u}_-(d,t)) = -\Gamma_3\dot{u}_M(t) + 2\Gamma_3\dot{u}_+(d,t), \tag{4}$$

where the displacement $u_M(t)$ of the mass M satisfies the continuity condition $u_M(t) = u_+(d,t) + u_-(d,t)$. A dot over a variable denotes time derivative.

Equation (4) describes the motion of the mass M in the potential $V(u_M)$ under an effective force $2\Gamma_3\dot{u}_+$ due to the incoming wave $u_+(d,t)$ with an effective damping expressed by the term $-\Gamma_3\dot{u}_M$. Equation (4) involves time derivatives but no space derivatives. This originates from the fact that the leads are perfectly dispersionless and lossless. (See Ref. [12] for a more detailed demonstration.)

The actual values of $u_+(d,t)$ and of $u_M(t)$ in equation (4) result from the incident wave $u_I(x = 0, t)$ and from the displacement $u_M(t)$ taken in earlier moments correspondingly to the transmission and multiple reflection at the junction point. Thus, when expressed in terms of the incident wave, the equation of motion (4) takes the following explicit form

$$M\ddot{u}_M(t) + \Gamma_3\dot{u}_M(t) + \frac{\partial V}{\partial u_M} = 2\Gamma_3\left\{\sum_{n=1}(-1)^{n+1} \times \left[\alpha_1\beta_3^{n-1}\dot{u}_I(0, t - (2n-1)d/c_3) + \beta_3^n\dot{u}_M(t - 2nd/c_3)\right]\right\} \tag{5}$$

which is a delayed differential equation with multiple lags [20] or, equivalently, a Volterra intergo-differential equation [21] with a singular memory kernel and with specific external perturbation.

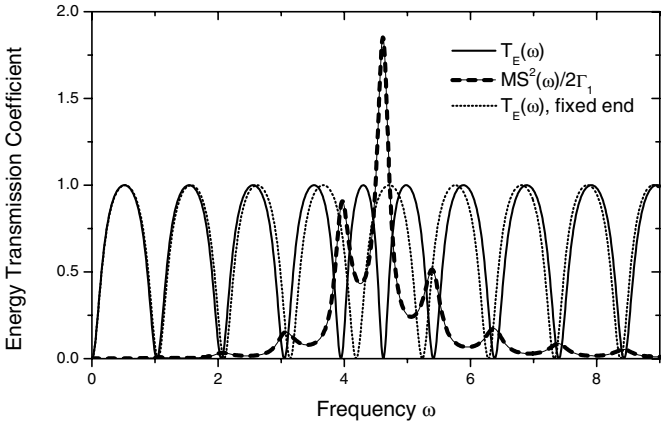

Fig. 2. Energy transmission coefficient T_E (Eq. (6a)) and energy of end mass M per energy of incident wave $MS^2/2\Gamma_1$ in harmonic limit of system of Figure 1 with parameters $M = 1$, $d = 3$, $c_1 = c_2 = c_3 = 1$, $\Gamma_1 = \Gamma_2 = \Gamma_3 = 1$ and potential of equation (1) with $a = 20$ and $b = 0$. Energy transmission coefficient for fixed end of resonator is shown for comparison.

3 Harmonic limit

If the amplitude of the incident wave is weak enough, the mass M oscillates in the vicinity of a minimum of the potential of equation (1). Then, the potential itself can be approximated by that of a harmonic oscillator $V(u_M) = \frac{1}{2}Au_M^2$. Remark that $A = a$ if $a > 0$ and $A = -2a$ if $a < 0$. The frequency domain analysis then can be applied to give the amplitudes $u_{T0}(\omega)$, $u_{R0}(\omega)$ of the sinusoidal transmitted and reflected waves as well as the amplitude $u_{M0}(\omega)$ of the oscillations of the mass M in the long time limit

$$u_{T0} = T(\omega)u_{I0} = \alpha_1\left\{1 + \alpha_3\frac{W(\omega)}{Z(\omega)}\right\}u_{I0}, \tag{6a}$$

$$u_{R0} = R(\omega)u_{I0} = \left\{\beta_1 + \alpha_1\alpha_3\frac{W(\omega)}{Z(\omega)}\right\}u_{I0}, \tag{6b}$$

$$u_{M0} = S(\omega)u_{I0} = \alpha_1\left\{\left[1 + \beta_3\frac{W(\omega)}{Z(\omega)}\right]\mathrm{e}^{-\mathrm{i}\omega d/c_3} + \frac{W(\omega)}{Z(\omega)}\mathrm{e}^{+\mathrm{i}\omega d/c_3}\right\}u_{I0}, \tag{6c}$$

where $W(\omega) = M\omega^2 - A + \mathrm{i}\omega\Gamma_3$ and $Z(\omega) = 2\mathrm{i}\omega\Gamma_3\mathrm{e}^{2\mathrm{i}\omega d/c_3} - W(\omega)[\beta_3 + \mathrm{e}^{2\mathrm{i}\omega d/c_3}]$. The quantities $T(\omega)$ and $R(\omega)$ are the amplitude transmission and reflection coefficients. The energy transmission and reflections coefficients are $T_E(\omega) = \frac{\Gamma_2}{\Gamma_1}|T(\omega)|^2$ and $R_E(\omega) = |R(\omega)|^2$. The general form of the transmission and reflection coefficients T and R (Eqs. (6a, 6b)) resembles that of reference [9]. The first term of each of these coefficients represents the straight and the second the resonant channel.

The specific boundary condition $M \to 0$, $A \to 0$ corresponds to the free end of the resonator as considered in references [4–7], whereas $M \to \infty$, $A \to \infty$ to the fixed end [8,9]. In both these limit cases the zeros of transmission are disposed equidistantly on the frequency axis [5]. In the general case the arrangement of the transmission

zeros is different. Figure 2 shows the energy transmission coefficient and the energy of the end mass M with respect to the energy of the incident wave $MS^2(\omega)/2\Gamma_1$ (see Eq. (6c)) as functions of frequency. The parameters of Figure 2 correspond to the harmonic approximation of the nonlinear system considered later. For comparison the transmission coefficient for the completely fixed end is also shown. It is seen that distances between zeros of transmission on the frequency axis are stretched in the vicinity of the resonance of the end mass. On the other hand zeros of transmission coincide with maxima of the amplitude u_{M0}.

4 Analogue electric circuit for the anharmonic system

In the general case of the potential of equation (1) the analysis of the system requires solution of the non-linear multi-delay equation equation (5), which is a particular case of the Volterra integro-differential equation. To our knowledge there are no efficient algorithms for the solution of such equations stable enough to give time series needed to establish the long time limit responses [21]. In the present work we have availed ourselves of the mechanical-electric analogy and have designed an electric circuit obeying the same equations of motion (Eqs. (2, 4) and (5)). The circuit is shown in Figure 3. The displacements are represented by charges and the velocities by currents. In particular, the displacement u_M of the mass M corresponds to the charge q on the capacitor C, which models the anharmonic string. The capacity C is nonlinear and depends on the charge in the way imposed by the explicit form of the potential $V(u_M)$

$$C(q) = \frac{q}{\mathrm{d}V(q)/\mathrm{d}q}\,. \tag{7}$$

The mass is modelled by an inductance, the semi-infinite media 1 and 2 by resistances Γ_1 and Γ_2, while the finite medium 3 by a transmission line of length d with the entrance impedance equal to Γ_3. The incident wave then corresponds to a voltage source with the electromotive force $F = 2\Gamma_1 \dot{u}_I$ equal numerically to the effective mechanical force exerted by the incident wave on the junction point. Time series of currents and voltages have been obtained with the use of the program SPICE. For comparison with earlier works a double-well potential, equation (1) with parameters $a = -10$ and $a = 100$ from references [12] and [19] has been used. At weak enough amplitudes of the incident sinusoidal wave the system has been checked to follow perfectly the behaviour predicted by the harmonic approximation (Eqs. (6), Fig. 2)

5 Characteristics of the nonlinear response

Whereas the response of the harmonic system to a sinusoidal perturbation in the long-time limit is always sinusoidal with the periodicity imposed by the perturbation,

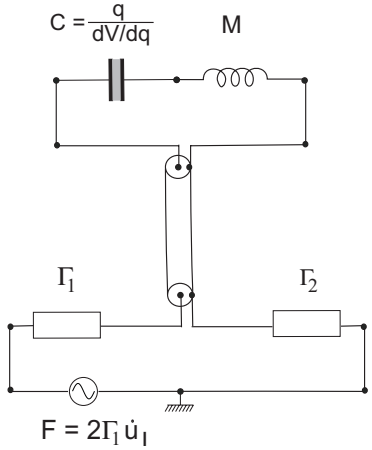

Fig. 3. Analogue electric circuit obeying equations of motion of model of Figure 1. Resistances Γ_1 and Γ_2 are numerically equal to wave impedances of medium 1 and medium 2 respectively.

there is generally a variety of cases possible in the presence of anharmonicity. In some ranges of parameters the response may show the same periodicity T_0 as the perturbation with, however, the wave forms modified by higher harmonics. Irregular, or chaotic response is marked by lack of any periodicity and by strange attractors in the phase space [20,22]. The region of chaos is sometimes interrupted by intermittent periodic areas, in which the periodicity T of the response is an integer multiple of the imposed periodicity $T = nT_0$ [22]. In other words, the system then generates subharmonics [12]. To characterise the kinds of behaviour mentioned we propose an aperiodicity index [23] here defined for the velocity $\dot{u}_M$

$$A(T) = \frac{1}{N}\sum_{i=n_0}^{n_0+N} \left(\dot{u}_M(t_i+T) - \dot{u}_M(t_i)\right)^2, \tag{8}$$

where n_0 is an arbitrarily chosen initial point in the time series $\dot{u}_M(t_i)$ and N is selected so as to cover several expected periods. Whenever T is a multiple of the period of $\dot{u}_M(t)$ the aperiodicity index vanishes. In the general case, the aperiodicity index has a minimum for a time interval $T = T_m$, which is called the minimal aperiodicity interval. The ratio T_m/T_0 is the period multiplicity. In the case of intermittency, there exists an integer n such that $A(nT_0) = 0$ and $A(T_0) > 0$. The period multiplicity then equals n. The use of the aperiodicity index allows one to distinguish the three types of response without a need for sophisticated analyses of attractors. This quantity may be also applied to time series obtained in experiments of different nature.

In what follows we compare the energy transmission coefficients and harmonics generation efficiencies with the corresponding aperiodicity index A and the period multiplicity T_m/T_0. This allows one to realize the influence of the anharmonic element onto propagation properties of the system.

Figure 4 shows the energy transmission coefficient $T_E(\omega)$ for the system of Figure 1 with the parameters

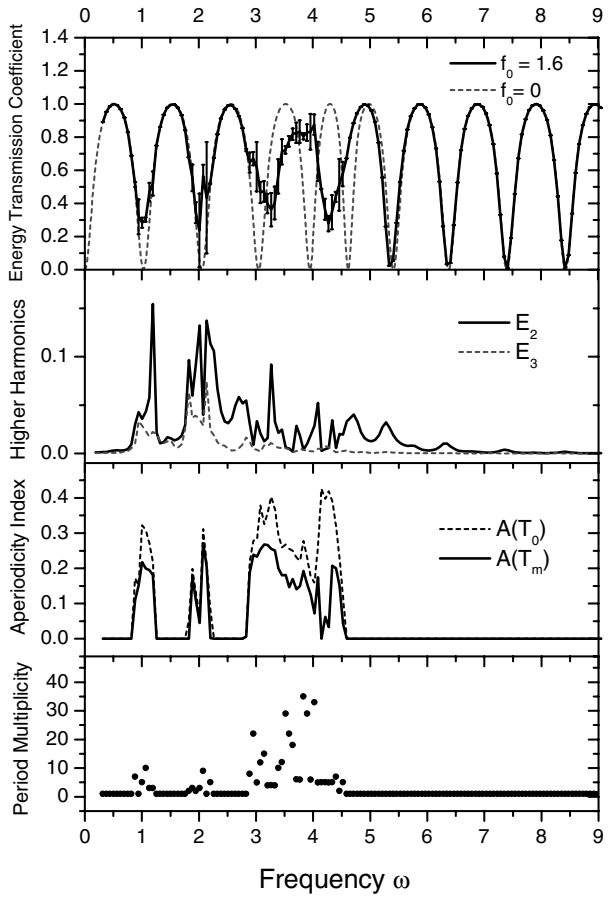

Fig. 4. Energy transmission coefficient $T_E(\omega)$ counted per minimal aperiodicity interval T_m, efficiencies E_2 and E_3 of second and third harmonic generation, aperiodicity indices and period multiplicity for system of Figure 1 with mass $M = 1$, resonator length $d = 3$, propagation velocities $c_1 = c_2 = c_3 = 1$, wave impedances $\Gamma_1 = \Gamma_2 = \Gamma_3 = 1$ and potential of equation (1) with $a = -10$ and $b = 100$. Effective force amplitude $f_0 = 1.6$. Dotted line $f_0 = 0$ shows energy transmission coefficient in harmonic approximation.

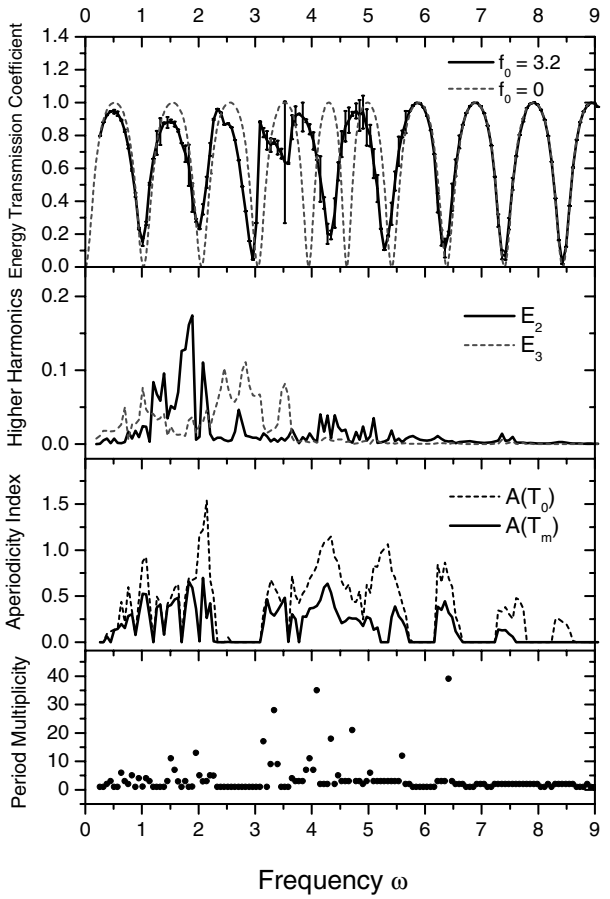

Fig. 5. Same as in Figure 3 but with $f_0 = 3.2$.

$M = 1$, $d = 3$, $\Gamma_1 = \Gamma_2 = \Gamma_3 = c_1 = c_2 = c_3 = 1$, and with the potential parameters $A = -10$ and $B = 100$. The initial state of the system corresponds to one of the minima of the potential. The amplitude f_0 of the effective force $F = 2\Gamma_1 \dot{u}_I$ exerted by the incident wave on the junction point is put 1.6. The energy transmission coefficient has been counted per the minimal aperiodicity period T_m. Whenever the transmitted wave is not periodic the energy transmission coefficient is a function of the initial point of the interval T_m and shows a distribution. The average transmission coefficient then is shown in Figure 4 along with its mean square error. The corresponding aperiodicity indices $A(T_0)$ and $A(T_m)$ as well as the period multiplicities are also shown. The most significant regions of aperiodic motion are visible close to and below the resonance frequency of the end mass M in the harmonic approximation, *i.e.* $\omega = \sqrt{-2a/M} = \sqrt{20}$. No clear evidence of intermittency can be discerned in Figure 4. Efficiency E_2 of the second harmonic generation shows clear maxima in the vicinity of the zeros of transmission. In these regions the system has a tendency to stop the fundamental and to transmit the second harmonic. Figure 5 shows the same quantities for still higher effective force $f_0 = 3.2$. Interesting is that the response of the system at higher frequencies practically coincides with the harmonic approximation. An apparent reason for that is that the effective damping then dominates over the potential and the mass M stays always close to a minimum of the potential.

The main effect of the anharmonicity is that the zeros of transmission and the total transmissions are lifted in some frequency ranges. In Figures 6 and 7 we report the energy transmission coefficients, second and third harmonic generation efficiency, aperiodicity indices and the period multiplicities as functions of the effective force amplitude f_0 for two frequencies: the total transmission frequency ($\omega = 1.5417125...$) and for the zero of transmission closest to the end mass resonance ($\omega = 4.618745...$). At lower frequencies the transmission coefficient varies weakly with increasing amplitude until very close to the onset of aperiodic motion, where it undergoes a rapid change (Fig. 6). Close to the resonance the zero of transmission is lifted at relatively weak amplitude the response of the system being still periodic with strong second harmonic (Fig. 7). A fairly large interval of intermittency ranging from $f_0 \approx 3.6$ to $f_0 \approx 4.1$ is found to be related to the period triplication. Since the transmission coefficient

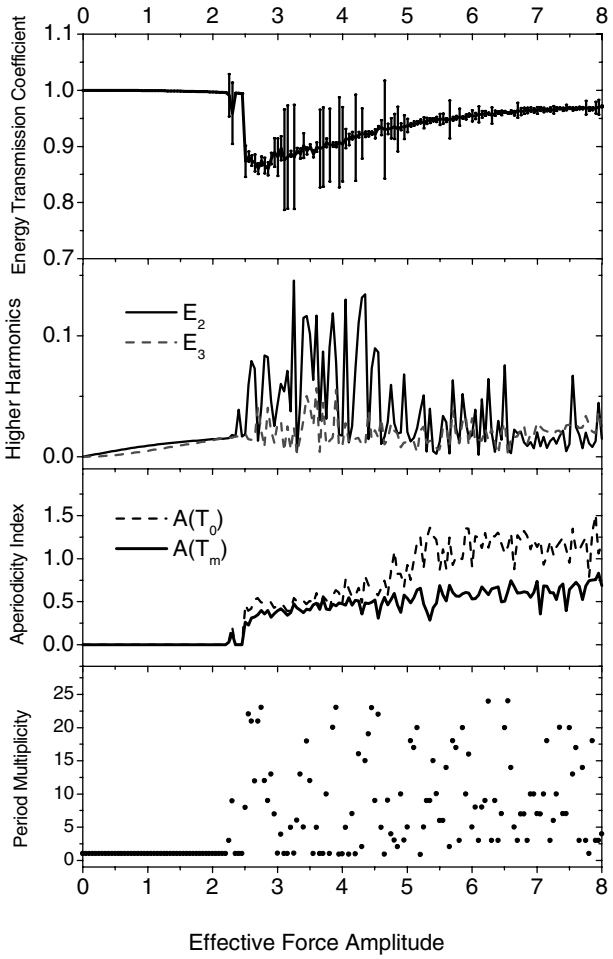

Fig. 6. Energy transmission coefficient, second and third harmonic generation efficiencies, aperiodicity indices and period multiplicity *versus* amplitude of applied force at frequency $\omega = 1.5417125...$ corresponding to total transmission in harmonic approximation (see Fig. 2).

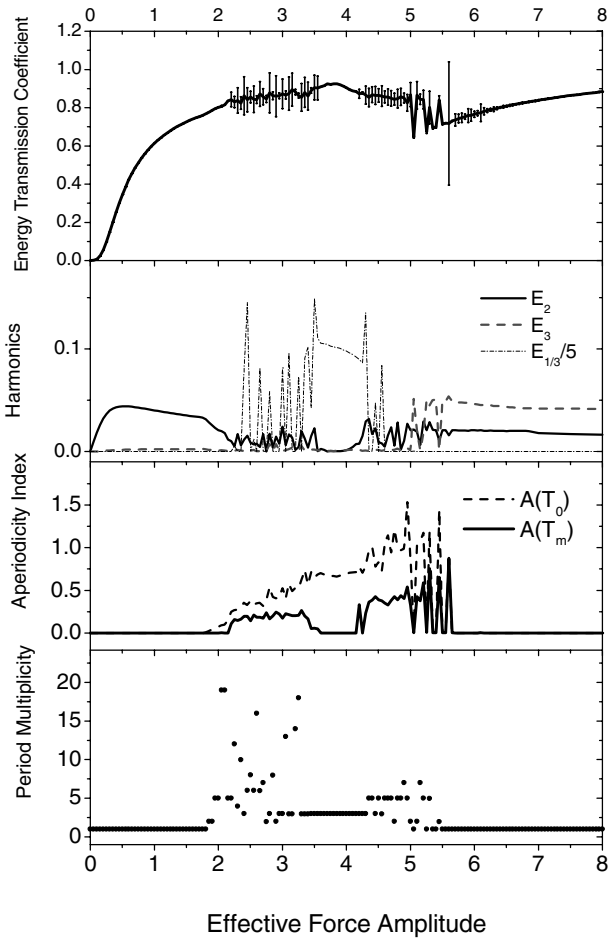

Fig. 7. Same as in Figure 4 but at frequency $\omega = 4.618745...$ corresponding in harmonic approximation to zero transmission closest to resonance of mass M. Efficiency $E_{1/3}$ of third subharmonic generation is also shown.

then surpasses 0.8 the system shows a tendency to transmit a strong third subharmonic, which is also shown in Figure 7.

No convincing evidence has been found of the Feigenbaum series of period doublings at the onset of the aperiodic motion. This is in contrast with analogous system equivalent to the usual Duffing oscillator [12,22] studied with the same methods where such a series was clearly visible. The reason for that may be that the present system governed by the delayed differential equation (Eq. (5)) does not follow at all the way to chaos by period doubling or that due to the multiple reflections at the junction point the time series studied here were too short with respect to the time intervals of aperiodic transient states preceding the onset of the true chaos. This question deserves to be treated in more detail in future.

6 Discussion

The results reported in the previous section concern a known and well-studied anharmonic potential (Duffing oscillator) placed in a system where the effective external perturbation acting on the mass M contains terms delayed in time (Eq. (5)). As a dynamical system the present model shows an infinite dimension of its phase space. Indeed, solution of its equation of motion requires the displacements and the velocities at all the length of the resonator. At first glance the same remark would also concern the semi-infinite leads "medium 1" and "medium 2". However, as it has been shown, the effect of these leads reduces to a damping term in the equation of motion, which corresponds to a thermal bath where energy is dissipated. The initial state of the leads may, of course, contain some waves traveling towards the junction. Such waves can be, however, incorporated into the incident wave or external excitation. The interplay of the external excitation (non-autonomous system) and dissipation underlies the chaotic behaviour observed in the model. In the general case of non dispersionless and non lossless leads the initial condition would be also needed for the semi-infinite parts. Thus, the effective dimension of the waveguide system depends crucially on the propagation properties of the waveguides themselves. In particular, a Duffing oscillator coupled exclusively to semi-infinite dispersionless and

lossless leads and excited by a sinusoidal external force is strictly equivalent to a damped Duffing oscillator and has three-dimensional phase space [12,19].

The problem as stated in this work resembles that considered by Farmer in reference [20]. The system is infinite dimensional and the relevant degrees of freedom cover an interval of finite length. A difference is that here the anharmonicity is strictly localised at one point, the end of the stub resonator, so that the delay part of equation (5) is linear, whereas the delay part of the Mackey and Glass equation (Eq. (14) of Ref. [20]) is explicitly nonlinear. Despite this difference the computational methods involving a discretisation of the interval proposed in reference [20] seem applicable. On the other hand we have already constructed a system of two coupled electric circuits the second of which represents the linearised equation needed to evaluate the Lyapunov exponents [24]. We are going to apply both techniques to the system considered here. Following the analogy with reference [20] we expect the chaotic attractors to show finite dimension, which may depend on parameters of the model. An interesting question is to what extent the "tangible" quantities such as those defined in Section 4 correlate with Lyapunov exponents and Lyapunov dimensions.

The quantities used in Section 4: the transmission coefficient together with its mean square error and the aperiodicity index together with the period multiplicity are well-adapted to analysis of time series obtained in spectroscopic experiments where sinusoidal measuring fields are used routinely. The present results show that a simple localized anharmonicity destroys the zeros of transmission and total transmission events especially when the nonlinear element provokes chaotic behaviour. The transmission coefficient then fluctuates in time, which makes the corresponding curve "thick", which is illustrated by the mean square error, Figures 4–7. A similar effect is expected in the presence of stochastic fluctuations of purely harmonic potential. In practice, however, the chaotic fluctuations seem to dominate in macroscopic waveguide systems, where the present results should apply in the best way.

Part of this work has been done during the stay of P.Z. at Laboratoire de Dynamique et Structure des Matériaux Moléculaires, CNRS ESA 8024, Université de Lille I, within contract PAST. The work is supported by grant No. 2 P03B 072 18 of The Committee for Scientific Researches (Poland).

References

1. M. Büttiker, Y. Imry, R. Landauer, Phys. Lett. A **96**, 365 (1983)
2. M. Büttiker, Y. Imry, M.Ya Azbel, Phys. Rev. A **30**, 1982 (1984)
3. R. Schuster, E, Buks, M. Heiblum, D. Mahalu, V. Umansky, H. Shtrikman, Nature **385**, 417 (1997)
4. T. Taniguchi, M.M. Büttiker, Phys. Rev. B **60**, 13814 (1999)
5. J.O. Vasseur, P.A. Deymier, L. Dobrzyński, B. Djafari-Rouhani, A. Akjouj, Phys. Rev. B **55**, 10434 (1997)
6. M.S. Kushwaha, A. Akjouj, B. Djafari-Rouhani, L. Dobrzyński, J.O. Vasseur, Solid State Comm. **106**, 659 (1998)
7. H. Al-Wash, A. Akjouj, B. Djafari-Rouhani, J.O. Vasseur, L. Dobrzyński, P.A. Deymier, Phys. Rev. B **59**, 8709 (1999)
8. W. Porod, Z. Shao, C.S. Lent, Appl. Phys. Lett. **61**, 1350 (1992)
9. H. Xu, W. Sheng, Phys. Rev. B **57**, 11903 (1998)
10. H.-W. Lee, Phys. Rev. Lett. **82**, 2358 (1999)
11. P. Zieliński, Z. Łodziana, T. Srokowski, Progr. Surf. Sci. **59**, 265 (1998)
12. P. Zieliński, Z. Łodziana, T. Srokowski, Eur. Phys. J. B **9**, 525 (1999)
13. L. Dobrzyński, Surf. Sci. Rep. **11**, 139 (1990)
14. See for example N. Brown, J. Biomechanics **26**, 59 (1993)
15. S.H. Bennett, B.W. Goetzman, J.M. Milstein, J.S. Pannu, J. Appl. Physiol. **80**, 1033 (1996)
16. G. Benedek, in *Dynamics of Gas-Surface Interaction*, Springer Series in Chemical Physics, edited by G. Benedek, U. Valbusa, Vol. **21** (Springer Berlin, 1982)
17. S.A. Adelmann, J.D. Doll, J. Chem. Phys. **61**, 4242 (1974)
18. G. Duffing, *Erzwungene Schwingungen bei Veraenderlicher Eigenfrequenz* (Viewig, Brauschseig, 1918)
19. W.-H. Steeb, W. Erig, A. Kunick, Phys. Lett. A **93**, 267 (1983).
20. See J.D. Farmer, Physica D, **4**, 366 (1982); for a problem with a single lag
21. See C.T.H. Baker, J. Comp. Appl. Math. **125**, 217 (2000); and references given therein for the state of art in numerical treatment of integro-differential equations
22. H.G. Schuster, *Chaos – An Introduction* (VCH, Weinheim, 1988), p. 52; also see G. Benettin, L. Galgani, A. Giorgilli, J.-M. Strelcyn, Meccanica **15**, 21 (1980)
23. A. Kułak, Z. Łodziana, T. Srokowski, W. Zając, P. Zieliński, Physica B **316-317**, 483 (2002)
24. K. Łukasik, A. Kułak, T. Srokowski, W. Zając, P. Zieliński, Materials Science and Engineering (submitted)